



# Approaching quantum-limited phase tracking with a large photon flux in a fiber Mach–Zehnder interferometer

Fang Liu<sup>1</sup> · Kaimin Zheng<sup>2</sup> · Liu Wang<sup>1</sup> · Chuan Xu<sup>2</sup> · Lidan Zhang<sup>2</sup> · TianXin Wang<sup>2</sup> · YuChang Liu<sup>1</sup> · Xiang Li<sup>1</sup> · Lijian Zhang<sup>2</sup> · Yong Zhang<sup>2</sup> · Min Xiao<sup>2,3</sup>

Received: 23 November 2020 / Accepted: 7 April 2021 / Published online: 3 May 2021  
© The Author(s), under exclusive licence to Springer Science+Business Media, LLC, part of Springer Nature 2021

## Abstract

The real-time phase tracking has a large number of applications in the precise measurement of various physical parameters. The classical limit of fiber phase tracking has been realized with homodyne detection under a low photon flux (typically  $\sim 10^6 \text{ s}^{-1}$ ). However, it is still difficult to approach the coherent state limit when measuring a weak phase fluctuation in real time by using a larger photon flux. In this work, we propose a fiber Mach–Zehnder system and experimentally demonstrate a nearly quantum-limited phase tracking with mean photon numbers of  $\sim 3.7 \times 10^{10} \text{ s}^{-1}$ . In the experiment, the input state is a continuous-mode coherent state and an adaptive Kalman filter is used to construct a phase-locked loop. We effectively track a very weak random phase varying between  $-0.07$  and  $+0.07$  radians, and the minimum mean-squared error is optimized to  $2.5 \times 10^{-5}$  which approaches the coherent state limit. Our method has potentially applications for fiber-based real-time sensing and measurements.

## 1 Introduction

An important task in quantum metrology is the estimation of phases in optical dynamics [1–12], the most compelling application being gravitational-wave detection [13–17]. For the measurements of constant phases, given  $N$  separated photons, the sensitivity of an optical measurement device scales as  $1/\sqrt{N}$  (i.e., shot-noise limit). Furthermore, the phase precision can be enhanced by using quantum lights [18–25]. Caves in 1981

---

✉ Yong Zhang  
zhangyong@nju.edu.cn

<sup>1</sup> Department of Physics, Nanjing Tech University, Nanjing 211816, China

<sup>2</sup> National Laboratory of Solid State Microstructures, College of Engineering and Applied Sciences, and School of Physics, Nanjing University, Nanjing 210093, China

<sup>3</sup> Department of Physics, University of Arkansas, Fayetteville, AR 72701, USA

initially proposed using squeezed-vacuum light to reach a sub-shot-noise sensitivity in a Mach–Zehnder interferometer (MZI) [1]. The first precision phase measurement using a MZI beyond the shot-noise limit was realized in 1987 [2]. Later, the phase precision of the interferometer was pushed to reach the Heisenberg limit [24, 25].

In many applications, e.g., atomic clocks, magnetometers and gravitational-wave detectors, the parameter that one wishes to measure varies in time [26–30]. For example, when estimating a stochastically varying phase, the central statistical problem is an estimation of the waveform [31–35]. The quantum Cramer-Rao bound imposes the fundamental limit to such waveform estimations [36–38]. In linear Gaussian model, Kalman filters (KFs) are optimized with minimum mean-squared error (MSE) for fast and causal estimations, which provide a full statistical description of the waveform [39]. To date, KFs have been experimentally implemented in various optical sensors to estimate the phase of a light beam [40–44]. Particularly, the combination of KFs with fiber interferometer has unique advantages, such as compact size, ease of deployment, immunity to electromagnetic disturbance, and long-distance sensing. Fiber-sensing systems have been widely deployed for strain, sound, and acceleration measurements in various environments [45–50]. However, the previous experiments demonstrate the quantum-limited phase tracking with homodyne detection under a low photon numbers [8, 32, 33, 44, 51]. For example, in a fiber homodyne system, the typical photon numbers of signal-carrying light are  $\sim 10^6 \text{ s}^{-1}$ , which is limited by the requirement of a strong local light. As well known, the measurement precision is proportional to the used photon numbers. One specific example is gravitational-wave detection, in which high laser power is applied to measure an extremely weak signal. With such a high photon flux, the classic noise is substantial and the electronic circuit is easy to be saturated. It is necessary to improve the performances of the optical and electronic systems to reach the limit. Similarly, it is still a great challenge to approach the theoretical limit by using a large photon flux in fiber MZI [33–35].

In this paper, we experimentally investigate the phase tracking of a continuous-wave coherent state in a fiber MZI, in which the photon flux can be enhanced by several orders of magnitudes in comparison to previous works [33, 34]. In addition, we can achieve high-precision estimation of waveforms that approach the theoretical limit by taking advantage of KFs. In this work, we firstly in theory demonstrate that the minimum phase variance of the KF estimation when tracking a stochastically varying waveform with a coherent light input of large photon flux in the interferometer. In the experiment, with a large photon flux  $|\alpha|^2 \sim 3.7 \times 10^{10} \text{ s}^{-1}$  for fiber interferometric detection, we effectively measure a very weak random phase varying between  $-0.07$  and  $+0.07$  radians and the minimum MSE of the phase estimator is  $2.5 \times 10^{-5}$ , which is close to the coherent state limit.

## 2 Theory

Here, we consider continuous-wave interferometric measurements (Fig. 1). The setup consists of a MZI, two detectors, and a data processor. And the attempt is to track continuously a stochastically varying phase  $\varphi(t)$ , by controlling the phase

$\Phi(t)$  in the other arm and detecting the photons in the two output beams [4]. Note that both beam splitters in Fig. 1 are 50/50. We inject a coherent field  $\hat{A} = \hat{a}e^{i\omega_0 t}$  at an optical carrier frequency of  $\omega_0$  and a vacuum state  $\hat{B} = \hat{b}e^{i\omega_0 t}$  into the MZI, here  $\hat{a}$  and  $\hat{b}$  denote annihilation operators for the input modes of the MZI. Using the linear operator method, we write  $\hat{a} = \alpha + \delta\hat{a}(t)$  and  $\hat{b} = \delta\hat{b}(t)$ , where  $\delta\hat{a}(t)$  and  $\delta\hat{b}(t)$  are the operator fluctuations. Using the matrix for a lossless 50/50 beam splitter, the output current of the balanced detector is given by

$$I(t) = |\alpha|^2 \cos(\varphi(t) - \Phi(t)) + |\alpha| \frac{dW(t)}{dt} \tag{1}$$

where  $W(t)$  denotes the quantum noise of the output current, modeled here as independent white Gaussian noise and satisfying  $\langle dW(t)dW(\tau) \rangle = \delta(t - \tau)(dt)^2$ . Usually, to achieve maximal measurement sensitivity for phase tracking, the relative phase of the two arms in MZI is taken to be  $\Phi(t) = \varphi_f(t) + \frac{\pi}{2}$ , with  $\varphi_f(t)$  being the filtered estimate of  $\varphi(t)$ . When the phase-locked loop functions well,  $\varphi_f(t)$  should be the real-time optimal estimate of  $\varphi(t)$  and the normalized current signal becomes

$$\eta(t) = \varphi(t) - \varphi_f(t) + \frac{dW(t)}{|\alpha|dt} \tag{2}$$

Considering that the random signal derives from an Ornstein–Uhlenbeck (OU) process, the stochastic waveform  $\varphi(t)$  is defined by

$$\frac{d\varphi(t)}{dt} = -\lambda\varphi(t) + \sqrt{\kappa} \frac{dV(t)}{dt} \tag{3}$$

where  $\lambda$  denotes the bandwidth of phase noise  $\varphi(t)$ ,  $\kappa/2\lambda$  the mean square variation of  $\Phi(t)$ , and  $dV(t)$  the classical Wiener increment satisfying  $\langle dV(t)dV(\tau) \rangle = \delta(t - \tau)(dt)^2$ .

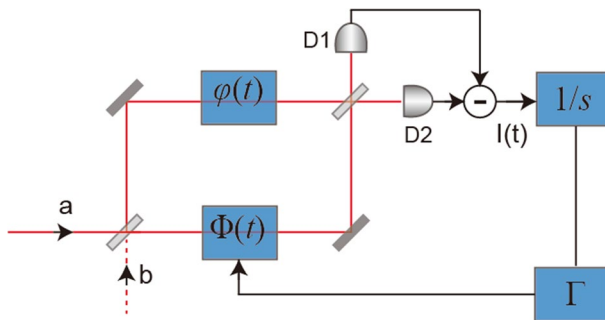


**Fig. 1** The theoretical scheme for adaptive measurement in a MZ interferometer. The random phase  $\varphi(t)$  is imposed on a coherent state carried by one arm of the MZI. D1 and D2 are photodetectors.  $I(t)$  is the photocurrent difference between the two outputs. The Kalman filter consists of an integrator ( $1/s$ ) with a Kalman gain ( $\Gamma$ ). The filter adjusts the phase of the arm labeled by  $\Phi(t)$  based on  $I(t)$

For time-continuous and linear Gaussian systems, the optimal estimator minimizing the MSE is provided by a Kalman-Bucy filter [52, 53], which satisfies the formula

$$\frac{d\varphi_f(t)}{dt} = -\lambda\varphi_f(t) + \Gamma\eta(t) \tag{4}$$

where  $\Gamma$  denotes the Kalman gain defined by  $\Gamma = |\alpha|^2\sigma^2(t)$ , with  $\sigma^2(t) = (\varphi(t) - \varphi_f(t))^2$  the MSE of the estimation. Solving Eq. (4) yields the estimator

$$\varphi_f(t) = \Gamma \int_{-\infty}^t e^{-\lambda(t-s)}\eta(s)ds \tag{5}$$

Here, we find the feedback phase changes with the Kalman gain. The Kalman-Bucy filter tells us how to obtain the minimal MSE, i.e., the optimal estimator. Note that  $\sigma^2(t)$  satisfies the equation

$$\frac{d\sigma^2(t)}{dt} = -2\lambda\sigma^2(t) - |\alpha|^2\sigma^4(t) + \kappa \tag{6}$$

In the steady state, Eq. (6) can be solved analytically to obtain the steady-state value

$$\sigma_s^2(t) = \frac{\lambda}{|\alpha|^2} \left( \sqrt{1 + \frac{\kappa|\alpha|^2}{\lambda^2}} - 1 \right) \tag{7}$$

In the condition of  $|\alpha|^2 \gg \lambda^2$ , we can get  $\sigma_s^2(t) \sim \sqrt{\frac{\kappa}{|\alpha|^2}}$ . Note that, from the estimate  $\varphi_f(t)$ , the phase of the local beam is adjusted adaptively using the feedback loop at the working point (Fig. 1). The optimal phase estimate is realized based on the obtained photodetector current processed by an integrator with a proportional gain. In a homodyne detection system with squeezed light, the minimum MSE of phase estimate is given as  $\sigma_s^2(t) \sim \sqrt{\frac{\kappa\bar{R}_{sq}}{4|\alpha|^2}}$ , where  $\bar{R}_{sq} \approx e^{-2r_m}$  with  $r_m$  being the squeezing parameter of input phase-squeezed state [8]. When using a -10 dB phase squeezing light, the MSE is  $\sigma_s^2(t) = \sqrt{\frac{\kappa}{40|\alpha|^2}}$ . In comparison, if using the Mach-Zehnder detection with coherent state in this work, the same MSE can be easily reached via increasing the photon flux by 40 times.

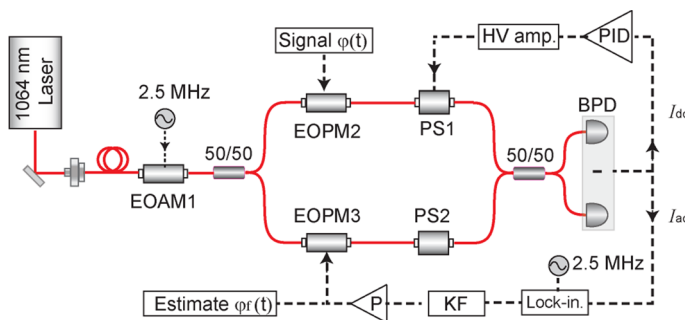
### 3 Experimental setup

Figure 2 shows our experimental setup. The MZI is illuminated by a continuous-wave Nd:YAG laser with a wavelength of 1064 nm. The laser beam has a narrow linewidth and low power fluctuations. At the beam output, an optical isolator is used to avoid optical feedback. The light is next coupled into a polarization-maintaining

fiber with 80% coupling efficiency. Before inputting into the MZI, the light is amplitude-modulated at 2.5 MHz using a waveguide EOM (waveguide modulator, EOspace) with a half-wave voltage of 3.5 V. This is a modulation technique for low-frequency phase measurement with a high signal-to-noise ratio, which effectively avoid low-frequency detection noise and to allow shot-noise-limited phase measurements at low frequencies [21]. The fiber MZI (Fig. 2) is based on two  $2 \times 2$  polarization-maintaining fiber couplers where the coupling ratios are 50/50. In the fiber arms, optical phase modulators (EOM2 and EOM3) are used to sense and track the phase varying at high rates. The fiber phase shifters PS1 driven by a piezoelectric transducer (PZT) (with half-wave voltages of 11 V at 1064 nm) is used to control the relative phase at low frequencies. Because it is critical to match the optical loss of fiber arms, fiber phase shifters PS2 is applied to balance the optical losses resulted from PS1, where loss difference of phase shifters is less than 0.1 dB. In our experiment, all the optical components in the system (Fig. 2) are polarization-maintaining fiber devices. Finally, the interference visibility is 99% and common-mode rejection ratio is 40 dB.

In the estimation experiments, the stochastic phase signal satisfied Eq. (3) is generated as following. A white Gaussian noise with 50 MHz bandwidth comes from digital signal generator (AFG3025, Tektronix) and passes a 1st-order low-pass filter with a cut-off frequency of  $\lambda/2\pi = 3$  kHz, then sends to EOM2. Due to the EOM working in its linear response range, the optical phase in one fiber arm will vary with an OU process consequently.

At the MZI output ports, the interference signal is detected by a balanced photon detector (BPD), which includes two InGaAs photodiodes (ETX500, JDS Uniphase Corporation) with the detector quantum efficiency of 90%. The dark noise of BPD is 20 dB below the vacuum noise with input optical power of 2.5 mW. Its low-frequency component (dc-100 Hz) is sent to a slow feedback loop to isolate the system from environmental disturbances, which stabilizes the relative phase  $\varphi$  of the two MZI arms at  $\pi/2$  for maximum sensitivity. Meanwhile, the high-frequency



**Fig. 2** The experimental setup for optical phase tracking of a random signal. The system consists of a fiber MZI, a low-noise balanced photon detector, a wide-bandwidth lock-in amplifier, and a Kalman filter for phase estimating. EOM: electro-optic modulator; 50/50: 50/50 fiber coupler; PS: fiber phase shifter; BPD: balanced photodetector; Lock-in: lock-in amplifier; KF, Kalman filter; P, proportion controller; HV amp: high-voltage amplifier

component ( $> 1$  MHz) is sent to a second phase-locked loop for the phase tracking. The output of BPD is demodulated by a Lock-in amplifier (HF2LI, Zurich Instruments), then the output current  $I(t)$  of MZI is measured. Next the implementation of the Kalman-Bucy filter will be discussed in detail. The theory of Kalman-Bucy filter provides the optimal estimator minimizing the MSE and the corresponding estimated phase when tracking an OU random signal. Given by Eq. (5) the feedback phase  $\varphi_f(t) = \Gamma \int_{-\infty}^t e^{-\lambda(t-s)} \eta(s) ds$ , the Kalman filter can be constructed by a 1st-order low-pass filter and a proportion controller, where the cutoff frequency is set as 3 kHz and the Kalman gain  $\Gamma$  is adjusted by the proportion controller. Specifically, we need to sweep the Kalman gain  $\Gamma$  to obtain the minimal MSE. Now the phase estimation term is generated and stored as an estimated phase  $\Phi'(t)$  for the next analysis. To study the performance of KF filter, the MZI output current  $I(t)$ , applied OU waveform  $\varphi(t)$  and KF estimated phase  $\varphi_f(t)$  are recorded by a signal oscilloscope with a sampling rate of 350 MHz (MSO-X 3034 T, KEYSIGHT).

## 4 Results and discussion

To study the performance of the phase tracking system, we implement a Kalman filter to construct the estimator in the fiber MZI. The applied Ornstein–Uhlenbeck waveform  $\varphi(t)$  and the Kalman filter estimates  $\varphi_f(t)$  are recorded by an oscilloscope in Fig. 3, where the random phase varies between  $-0.07$  and  $+0.07$  radians with a recorded time of 5 ms. During the tracking process, the filter tracks are well monitored with little time delay when the random phase varies in real time. Meanwhile, the output current of the interferometer is kept near the zero point, indicating that the relative phase between the two arms is well maintained at the working point of  $\pi/2$ . In the experiment, the amplitude  $|\alpha|^2$  of the coherent beam, the amplitude factor  $\kappa$  of the phase variance, and phase noise bandwidth  $\lambda$  are  $3.1 \times 10^{10} \text{ s}^{-1}$ ,  $14 \text{ rad/s}$ , and  $1.89 \times 10^4 \text{ rad/s}$ , respectively. We remark that the photon flux includes only the sideband modes because the carrier is removed after demodulation by lock-in amplifier.

Furthermore, to validate the performance of the KF, we investigate the MSE of the estimation by adjusting the input coherent light to change the photon flux  $|\alpha|^2$ . Figure 4 gives the measured MSE of the phase estimate as a function of the photon flux. The photon flux ranges  $6 \times 10^9 \text{ s}^{-1}$  to  $3.7 \times 10^{10} \text{ s}^{-1}$  and the values of  $\kappa$  and  $\lambda$  are the same as used in Fig. 3. Note that, we adjust the Kalman gain to obtain optimal tracking results when changing the photon flux in the experiment. The red solid line is the coherent state limit given by adaptive Kalman filter, where minimum estimated MSE is  $\sigma_s^2(t) = \sqrt{\frac{\kappa}{|\alpha|^2}}$  and  $|\alpha|^2$  is the total photon flux. Considering the quantum efficiency of the photodetector is 90%, the black dash line gives the theoretical limit of the KF which is the same as the coherent state limit except the effective photo flux. When the corresponding photon numbers of coherent light is  $3.7 \times 10^{10} \text{ s}^{-1}$  in Fig. 4, the experimental MSE for the tracking process is  $2.5 \times 10^{-5}$ , which is quite close to the theoretical value.

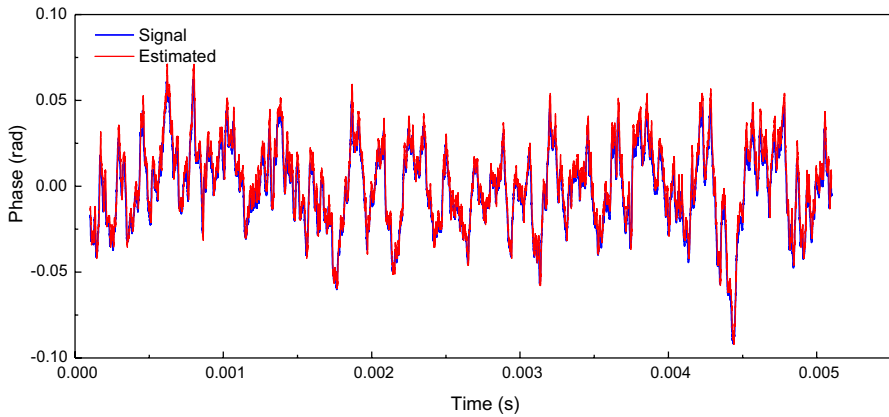


**Fig. 3** Time traces of the OU random signal with a 3 kHz bandwidth and the corresponding estimation result. The amplitude  $|\alpha|^2$  of the coherent beam is  $3.1 \times 10^{10} \text{ s}^{-1}$ , the amplitude factor  $\kappa$  of the phase variance is 14 rad/s, and filter bandwidth is  $\lambda 1.89 \times 10^4 \text{ rad/s}$

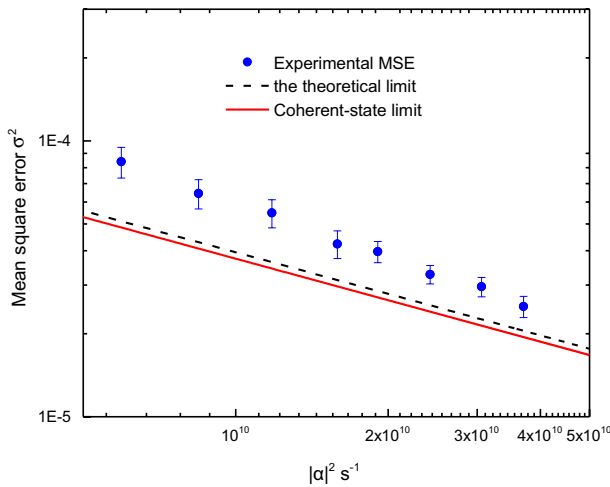


**Fig. 4** Dependence of MSE  $\sigma^2$  on optical power photon flux of coherent light  $|\alpha|^2$ . The blue dots are experimental results, the black dashed curves are the theoretical limit considering the experimental imperfections, the red solid curves are the coherent state limit (Color figure online)

To further analyze the difference between theory and experiment, we measure the noise spectrum aided by a Fourier-frequency analyzer (Fig. 5). When no signals imposed to the MZI and the slow feedback loop is locked, the total noise floor of the system is measured and shown by gray line in Fig. 5. Then Ornstein–Uhlenbeck signal with a corner frequency of 3 kHz is implemented, its frequency response is given by green curve. In the next, the feedback loop of the fiber MZI is locked on and the performance of Kalman filter is analyzed. In the range from 80 Hz to 5 kHz, the frequency response of the KF estimator well

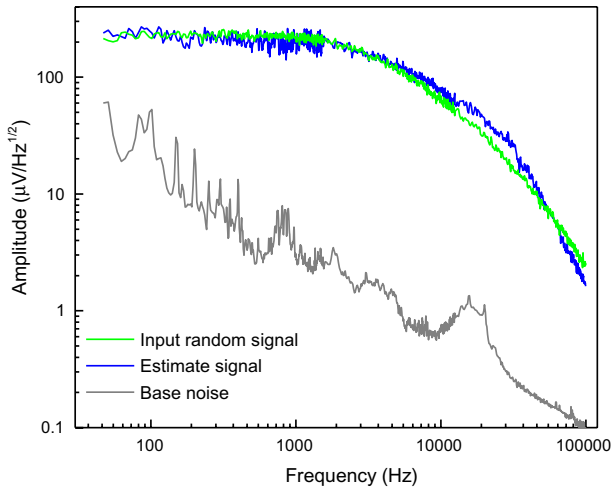


**Fig. 5** Noise spectrum analysis. The green curve shows the frequency response to Ornstein–Uhlenbeck signal with a corner frequency of 3 kHz. The respective tracked spectrum is plotted in blue line. The gray line gives the total noise floor of the system without OU signal. Here, the  $|\alpha|^2$ ,  $\kappa$  and  $\lambda$  are  $1.9 \times 10^{10} \text{ s}^{-1}$ ,  $14 \text{ rad/s}$ , and  $1.89 \times 10^4 \text{ rad/s}$ , respectively (Color figure online)

coincides with the random phase signal. At frequencies of about several tens of hertz, the total noise floor of the system is pretty large with no clear quantum-limited characteristics because of the vibration noise and the optical power noise of the laser beam. At around 10 kHz, being limited by the gain bandwidth product of the estimator loop, there is a slight discrepancy between the KF estimator and the input OU signal. For low-frequency measurements, our methods in which the local oscillator field is amplitude-modulated in the MHz range and is then demodulated can effectively mitigate both electronic and optical noise in the kilohertz frequency range. However, further laser power stabilization and vibration isolation will be needed to achieve quantum-limited phase measurement at frequencies below 100 Hz.

## 5 Conclusions

We have proposed and experimentally demonstrated high-precision estimation of a time-varying phase in a fiber MZ interferometer scheme. Under a larger photon flux  $|\alpha|^2 \sim 3.7 \times 10^{10} \text{ s}^{-1}$ , a very weak random phase varying between  $-0.07$  and  $+0.07$  radians is estimated and the MSE of the phase estimator is optimized to  $2.5 \times 10^{-5}$ , which approaches the coherent state limit. Compared with adaptive homodyne detection, our MZI system could significantly improve the MSE limit of estimators by employing high mean photon numbers. Our method can be further extended to quantum-enhanced phase tracking [54], which has potentially applications for fiber-based real-time sensing and measurements.



**Acknowledgments** The authors would like to thank Hidehiro Yonezawa, Lisheng Chen and Liufeng Li for illuminating discussions on this work. This research was supported by the National Key R&D Program of China (2017YFA0303703), Fundamental Research Funds for the Central Universities (021314380105), and the National Science Foundation of China (Grant No. 61605072, 61771236.).

## Declarations

**Conflict of interest** The authors declare no conflicts of interest.

## References

1. Caves, C.M.: Quantum-mechanical noise in an interferometer. *Phys. Rev. D* **23**, 1693–1708 (1981)
2. Xiao, M., Wu, L.A., Kimble, H.J.: Precision measurement beyond the shot-noise limit. *Phys. Rev. Lett.* **59**, 278–281 (1987)
3. Grangier, P., Slusher, R.E., Yurke, B., LaPorta, A.: Squeezed-light-enhanced polarization interferometer. *Phys. Rev. Lett.* **59**, 2153–2156 (1987)
4. Berry, D.W., Wiseman, H.M.: Adaptive quantum measurements of a continuously varying phase. *Phys. Rev. A* **65**, 043803 (2002)
5. Giovannetti, V., Lloyd, S., Maccone, L.: Advances in quantum metrology. *Nat. Photonics* **5**, 222–229 (2011)
6. Tsang, M., Wiseman, H.M., Caves, C.M.: Fundamental quantum limit to waveform estimation. *Phys. Rev. Lett.* **106**, 090401 (2011)
7. Joo, J., Munro, W.J., Spiller, T.P.: Quantum metrology with entangled coherent states. *Phys. Rev. Lett.* **107**, 083601 (2011)
8. Yonezawa, H., Nakane, D., Wheatley, T.A., Iwasawa, K., Takeda, S., Arao, H., Ohki, K., Tsumura, K., Berry, D.W., Ralph, T.C., Wiseman, H.M., Huntington, E.H., Furusawa, A.: Quantum-enhanced optical-phase tracking. *Science* **337**, 1514–1517 (2012)
9. Chiang, C.-F.: Selecting efficient phase estimation with constant-precision phase shift operators. *Quantum Inf. Process.* **13**, 415–428 (2014)
10. Berni, A.A., Gehring, T., Nielsen, B.M., Händchen, V., Paris, M.G.A., Andersen, U.L.: Ab initio quantum-enhanced optical phase estimation using real-time feedback control. *Nat. Photonics* **9**, 577–581 (2015)
11. Meher, N., Sivakumar, S.: Enhancing phase sensitivity with number state filtered coherent states. *Quantum Inf. Process.* **19**, 51 (2019)
12. Zheng, K., Xu, H., Zhang, A., Ning, X., Zhang, L.: Ab initio phase estimation at the shot noise limit with on-off measurement. *Quantum Inf. Process.* **18**, 329 (2019)
13. Gea-Banacloche, J., Leuchs, G.: Squeezed states for interferometric gravitational-wave detectors. *J. Mod. Opt.* **34**, 793–811 (1987)
14. Goda, K., Miyakawa, O., Mikhailov, E.E., Saraf, S., Adhikari, R., McKenzie, K., Ward, R., Vass, S., Weinstein, A.J., Mavalvala, N.: A quantum-enhanced prototype gravitational-wave detector. *Nat. Phys.* **4**, 472–476 (2008)
15. Grote, H., Danzmann, K., Dooley, K.L., Schnabel, R., Slutsky, J., Vahlbruch, H.: First long-term application of squeezed states of light in a gravitational-wave observatory. *Phys. Rev. Lett.* **110**, 181101 (2013)
16. LIGO Scientific Collaboration and Virgo Collaboration: Observation of gravitational waves from a binary black hole merger. *Phys. Rev. Lett.* **116**, 061102 (2016)
17. LIGO Scientific Collaboration and Virgo Collaboration: GW170817: Observation of Gravitational waves from a binary neutron star inspiral. *Phys. Rev. Lett.* **119**, 161101 (2017)
18. Otterstrom, N., Pooser, R.C., Lawrie, B.J.: Nonlinear optical magnetometry with accessible in situ optical squeezing. *Opt. Lett.* **39**, 6533–6536 (2014)
19. Sun, H., Liu, Z., Liu, K., Yang, R., Zhang, J., Gao, J.: Experimental demonstration of a displacement measurement of an optical beam beyond the quantum noise limit. *Chin. Phys. Lett.* **31**, 084202 (2014)
20. Hudelist, F., Kong, J., Liu, C., Jing, J., Ou, Z.Y., Zhang, W.: Quantum metrology with parametric amplifier-based photon correlation interferometers. *Nat. Commun.* **5**, 3049 (2014)

21. Liu, F., Zhou, Y., Yu, J., Guo, J., Wu, Y., Xiao, S., Wei, D., Zhang, Y., Jia, X., Xiao, M.: Squeezing-enhanced fiber Mach-zehnder interferometer for low-frequency phase measurement. *Appl. Phys. Lett.* **110**, 021106 (2017)
22. Lawrie, B.J., Lett, P.D., Marino, A.M., Pooser, R.C.: Quantum sensing with squeezed light. *ACS Photonics* **6**, 1307–1318 (2019)
23. Liu, S., Lou, Y., Jing, J.: Interference-induced quantum squeezing enhancement in a two-beam phase-sensitive amplifier. *Phys. Rev. Lett.* **123**, 113602 (2019)
24. Giovannetti, V., Lloyd, S., Maccone, L.: Quantum-enhanced measurements: Beating the standard quantum limit. *Science* **306**, 1330 (2004)
25. Nagata, T., Okamoto, R., Brien, J.L., Sasaki, K., Takeuchi, S.: Beating the standard quantum limit with four-entangled photons. *Science* **316**, 726 (2007)
26. Ludlow, A.D., Boyd, M.M., Ye, J., Peik, E., Schmidt, P.O.: Optical atomic clocks. *Rev. Mod. Phys.* **87**, 637–701 (2015)
27. Wolfgramm, F., Cerè, A., Beduini, F.A., Predojević, A., Koschorreck, M., Mitchell, M.W.: Squeezed-light optical magnetometry. *Phys. Rev. Lett.* **105**, 053601 (2010)
28. Taylor, M.A., Janousek, J., Daria, V., Knittel, J., Hage, B., Bachor, H.-A., Bowen, W.P.: Biological measurement beyond the quantum limit. *Nat. Photonics* **7**, 229–233 (2013)
29. Feng, L., Zhang, M., Zhou, Z., Li, M., Xiong, X., Yu, L., Shi, B., Guo, G., Dai, D., Ren, X., Guo, G.: On-chip coherent conversion of photonic quantum entanglement between different degrees of freedom. *Nat. Commun.* **7**, 11985 (2016)
30. The LIGO Scientific Collaboration: Enhanced sensitivity of the LIGO gravitational wave detector by using squeezed states of light. *Nat. Photonics* **7**, 613–619 (2013)
31. Armen, M.A., Au, J.K., Stockton, J.K., Doherty, A.C., Mabuchi, H.: Adaptive homodyne measurement of optical phase. *Phys. Rev. Lett.* **89**, 133602 (2002)
32. Iwasawa, K., Makino, K., Yonezawa, H., Tsang, M., Davidovic, A., Huntington, E., Furusawa, A.: Quantum-limited mirror-motion estimation. *Phys. Rev. Lett.* **111**, 163602 (2013)
33. Zhang, L., Zheng, K., Liu, F., Zhao, W., Tang, L., Yonezawa, H., Zhang, L., Zhang, Y., Xiao, M.: Quantum-limited fiber-optic phase tracking beyond pi range. *Opt. Express* **27**, 2327–2334 (2019)
34. Cimini, V., Mellini, M., Rampioni, G., Sbroscia, M., Leoni, L., Barbieri, M., Gianani, I.: Adaptive tracking of enzymatic reactions with quantum light. *Opt. Exp.* **27**, 35245–35256 (2019)
35. Cimini, V., Gianani, I., Ruggiero, L., Gasperi, T., Sbroscia, M., Rocca, E., Tofani, D., Bruni, F., Ricci, M.A., Barbieri, M.: Quantum sensing for dynamical tracking of chemical processes. *Phys. Rev. A* **99**, 053817 (2019)
36. Berry, D.W., Tsang, M., Hall, M.J.W., Wiseman, H.M.: Quantum Bell-Ziv-zakai bounds and heisenberg limits for waveform estimation. *Phys. Rev. X* **5**, 031018 (2015)
37. Berry, D.W., Hall, M.J.W., Wiseman, H.M.: Stochastic heisenberg limit: optimal estimation of a fluctuating phase. *Phys. Rev. Lett.* **111**, 113601 (2013)
38. Dinani, H.T., Berry, D.W.: Adaptive estimation of a time-varying phase with a power-law spectrum via continuous squeezed states. *Phys. Rev. A* **95**, 063821 (2017)
39. Cooper, W.S.: Use of optimal estimation theory, in particular the Kalman filter, in data analysis and signal processing. *Rev. Sci. Instrum.* **57**, 2862–2869 (1986)
40. Beker, M.G., Bertolini, A., van den Brand, J.F., Bulten, H.J., Hennes, E., Rabeling, D.S.: State observers and Kalman filtering for high performance vibration isolation systems. *Rev. Sci. Instrum.* **85**, 034501 (2014)
41. Marshall, T., Szafraniec, B., Nebendahl, B.: Kalman filter carrier and polarization-state tracking. *Opt. Lett.* **35**, 2203–2205 (2010)
42. Jimenez-Martinez, R., Kolodynski, J., Troullinou, C., Lucivero, V.G., Kong, J., Mitchell, M.W.: Signal tracking beyond the time resolution of an atomic sensor by kalman filtering. *Phys. Rev. Lett.* **120**, 040503 (2018)
43. Dubey, S.U., Dubey, P.K., Rajagopalan, S., Sharma, S.J.: Real-time implementation of Kalman filter to improve accuracy in the measurement of time of flight in an ultrasonic pulse-echo setup. *Rev. Sci. Instrum.* **90**, 025105 (2019)
44. Wieczorek, W., Hofer, S.G., Hoelscher-Obermaier, J., Riedinger, R., Hammerer, K., Aspelmeyer, M.: Optimal state estimation for cavity optomechanical systems. *Phys. Rev. Lett.* **114**, 223601 (2015)
45. Lee, B.: Review of the present status of optical fiber sensors. *Opt. Fiber Technol.* **9**, 57–79 (2003)
46. Mauranyapin, N.P., Madsen, L.S., Taylor, M.A., Waleed, M., Bowen, W.P.: Evanescent single-molecule biosensing with quantum-limited precision. *Nat. Photonics* **11**, 477–481 (2017)

47. Wang, X., Chen, S., Du, Z., Wang, X., Shi, C., Chen, J.: Experimental study of some key issues on fiber-optic interferometric sensors detecting weak magnetic field. *IEEE Sens. J.* **8**, 1173–1179 (2008)
48. McRae, T.G., Ngo, S., Shaddock, D.A., Hsu, M.T.L., Gray, M.B.: Frequency stabilization for space-based missions using optical fiber interferometry. *Opt. Lett.* **38**, 278–280 (2013)
49. Mehmet, M., Eberle, T., Steinlechner, S., Vahlbruch, H., Schnabel, R.: Demonstration of a quantum-enhanced fiber Sagnac interferometer. *Opt. Lett.* **35**, 1665–1667 (2010)
50. Huo, M., Qin, J., Cheng, J., Yan, Z., Qin, Z., Su, X., Jia, X., Xie, C., Peng, K.: Deterministic quantum teleportation through fiber channels. *Sci. Adv.* **4**, eaas9401 (2018)
51. Ben-Aryeh, Y.: Phase estimation by photon counting measurements in the output of a linear Mach-Zehnder interferometer. *J. Opt. Soc. Am. B-Opt. Phys.* **29**, 2754–2764 (2012)
52. Tsang, M., Shapiro, J.H., Lloyd, S.: Quantum theory of optical temporal phase and instantaneous frequency II Continuous-time limit and state-variable approach to phase-locked loop design. *Phys. Rev. A* **79**(5), 053843 (2009)
53. Laverick, K.T., Wiseman, H.M., Dinani, H.T., Berry, D.W.: Adaptive estimation of a time-varying phase with coherent states: Smoothing can give an unbounded improvement over filtering. *Phys. Rev. A* **97**, 042334 (2018)
54. Xu, C., Zhang, L., Huang, S., Ma, T., Liu, F., Yonezawa, H., Zhang, Y., Xiao, M.: Sensing and tracking enhanced by quantum squeezing. *Photonics Res.* **7**, A14–A26 (2019)

**Publisher's Note** Springer Nature remains neutral with regard to jurisdictional claims in published maps and institutional affiliations.